Power Loss Associated with Conducting and Superconducting Rough Interfaces

Christopher L. Holloway, *Member, IEEE*, and Edward F. Kuester, *Fellow, IEEE*

***Abstract*—In recent work, a generalized impedance boundary condition for two-dimensional conducting rough interfaces was derived. In this study, the impedance boundary condition is used to calculate the power loss associated with conducting rough interfaces. Results for two-dimensional conducting and superconducting roughness profiles are shown in this paper, and comparisons to other results in the literature are given. The importance of these roughness effects in microwave and millimeter-wave integrated circuits is also discussed. Suggestions are made to extend this study to three-dimensional random rough interfaces.**

***Index Terms*—Impedance boundary condition, power loss, rough surfaces, superconducting rough interface.**

I. Introduction

THE standard procedure for manufacturing microwave and millimeter-wave integrated circuits (MIMICs) involves a cycle of design analysis, production, and testing. This procedure is repeated until the circuit meets all designated specifications. As MIMICs become more and more complicated and expensive to build, a need evolves to eliminate as many loops as possible in this process. One important design concern is power loss associated with the circuit, especially near its resonance frequencies.

There are three basic types of loss in planar circuits: radiation, dielectric, and conductor loss. Radiation loss, such as excitation of surface wave modes along the dielectric substrate, is only significant at discontinuities in planar circuits. This loss can be lessened by reducing the substrate height, which decreases the amplitudes and number of these modes. Dielectric loss has been analyzed in the past [1]–[4], and in most MIMIC applications, this loss is small compared to the total loss. Thus, the dominant loss mechanism is the conductor loss, which is the emphasis of this paper.

The conventional way to determine the conductor loss is to use a perturbation approach. This method assumes that the fields of a line with small conductor loss are perturbed only slightly from the fields of the corresponding lossless line. The attenuation caused by the conductor loss is then

$$\alpha_c = \frac{1}{2Z_o|I|^2} R_s \oint_s |\mathbf{J}|^2 \, dl$$

Manuscript received November 6, 1997.

C. L. Holloway was with the U.S. Department of Commerce, Boulder Laboratories, Institute for Telecommunication Sciences, Boulder, CO 80303 USA. He is now with the National Institute of Standards and Technology, Boulder, CO 80303 USA.

E. F. Kuester is with the Department of Electrical and Computer Engineering, University of Colorado at Boulder, Boulder, CO 80309-0425 USA.

Publisher Item Identifier S 0018-9480(00)08731-7.

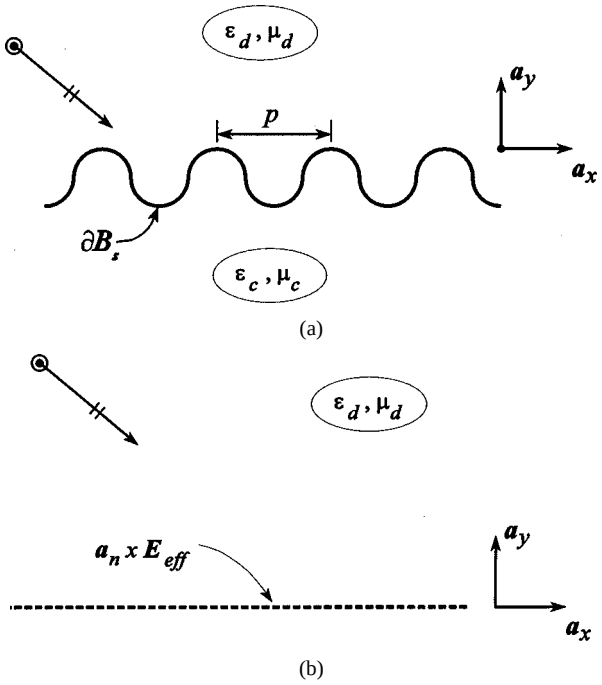

Fig. 1. (a) Geometry of a rough conducting interface. (b) Flat interface where the equivalent boundary condition is applied to the effective field.

where $\mathbf{J}$ is the surface current density of a perfectly conducting line, R_s is the standard Leontovich surface impedance [5], [6], and Z_o is the characteristic impedance.

This conventional approach is limited to situations where the Leontovich condition is valid. If the thickness of the conductor becomes comparable to the skin depth δ, the Leontovich condition breaks down. Also, if the radius of curvature of the conductors is on the same order as (or smaller than) the skin depth, such as in the presence of sharp edges and corners, or if the conductor surface is rough, the Leontovich condition again fails. The purpose of this paper is to study the effects of surface roughness on loss mechanisms associated with planar circuits. The effects of the shape of the conductor edges have been investigated separately in [7] and [8]. Reference [7] also gives a generalized surface impedance boundary condition for thin conductors.

As the operating frequency of MIMICs is pushed higher and higher, any type of surface blemish on the conductor can become important. The effect of the surface roughness on the power loss is explained by referring to Fig. 1(a). When the roughness dimensions are small compared to the skin depth, only a small percent of the total current "sees" the roughness and, as a result, one should not expect there to be much additional power loss above that of a smooth conductor. However, as the frequency increases, the skin depth decreases and begins to approach the

roughness dimensions. In this case, the current and fields in the conductor are forced near the surface, and a larger fraction of the total current "sees" the roughness, forcing the current to follow a different path than when roughness is absent. Consequently, more power dissipation over that of the smooth conductor is to be expected.

These blemishes can arise from different sources. The first is the condition of the substrate. If the substrate is rough, then the conductor/substrate interface will itself be rough. There are basically three different materials used for substrates in MIMIC applications: PTFE ($2 < \epsilon_r < 7$), Al_2O_3 ($\epsilon_r \simeq 10$) and GaAs ($\epsilon_r \simeq 12.9$). Each of these has different roughness features. PTFE and unpolished Al_2O_3 have rms roughness dimensions on the order of 0.3–1.0 μm [1], [9]. However, Al_2O_3 can be polished to roughness dimensions on the order of 0.04 μm [10], [11]. GaAs is the smoothest of the three materials and can be polished optically smooth, with roughness on the order of 50–100 Å.

Surface roughness can also originate from the way in which the metal is deposited onto the substrate. On PTFE and Al_2O_3 substrates, copper is usually deposited by either a rolled-copper or electrodepositing process. Rolled copper usually has a smoother metal/substrate and metal/air interface than that which results from electrodepositing. For rolled copper, the roughness dimensions are on the order of 0.1 μm for the metal/substrate interface and on the order of 1 μm for the metal/air interface. Electrodepositing results in roughness dimensions on the order of 0.5 and 5.0 μm for the two interfaces, respectively. For GaAs, substrate metal is usually deposited by either electroplating or evaporation. Since GaAs is usually polished, the metal/substrate interface is optically smooth, and the only roughness occurs at the metal/air interface. Here, electroplating results in roughness dimensions on the order of 0.1–0.4 μm, while for evaporation, the metal/air interface is optically smooth.

The goal of this paper is to predict the additional power loss dissipated in a conductor with a rough surface compared to that dissipated in the same conductor with a smooth boundary. Our analysis relies on previous work that characterizes a rough surface by a generalized impedance boundary condition (GIBC) for the effective (or average) fields outside the conductor [12]. It should be noted that other recent work has appeared in which a rough conducting surface is described by an impedance boundary condition (see, e.g., [13]–[15]). While this latter work also allows the effect of the rough surface to be accounted for without the need to find the fields in the conductor, it differs from the approach in [12] in that the surface impedance is a function of position, varying on the same length scale as does the rough surface. While this does allow for prediction of higher order Floquet modes and Bragg-type effects, it also means that practical usage of the impedance condition will require very fine spatial resolution of the fields in numerical solutions if the roughness scale is small. Our approach, on the other hand, is limited to the case when the roughness dimensions are small compared to a wavelength and all other physical dimensions of the structure, but also allows much simpler and cheaper numerical solutions since the field does not have to be solved for in over-extreme detail.

II. Power Loss in the Conductor

In previous work [12], the asymptotic technique of homogenization was used to derive the following GIBC for a two-dimensional periodic interface between a dielectric and a highly conducting medium [see Fig. 1(a)]:

$$\mathbf{a}_y \times \mathbf{E}(\mathbf{r}_o) = j\omega p[\mathbf{a}_x \alpha_{mx} B_x(\mathbf{r}_o) + \mathbf{a}_z \alpha_{mz} B_z(\mathbf{r}_o)] - p\alpha_{ey} \mathbf{a}_y \times \nabla_r E_y(\mathbf{r}_o) \quad (1)$$

where p is the period of the roughness and $\mathbf{r}_o = \mathbf{a}_x x + \mathbf{a}_z z$. The coefficients ($\alpha_{ey}$, α_{mx}, α_{mz}) in this boundary condition can be interpreted as normalized electric and magnetic polarizability densities; they are given in [12] and will be defined here as needed. The electric polarizability density α_{ey} is a pure real quantity and, as will be shown below, does not contribute to the power loss. On the other hand, the magnetic polarizability densities (α_{mx} and α_{mz}) are, in general, complex, and do contribute to the power loss.

It was demonstrated in [12] and [16] that the electromagnetic field scattered from a rough periodic interface can be approximated (at least sufficiently far from the rough surface) by applying the GIBC given in (1) to a certain effective smooth surface [as shown in Fig. 1(b)]. This equivalent boundary condition along with Maxwell's equations are all that is needed to determine electromagnetic interaction with a rough interface if the fine details of the field near the surface are not needed. The power dissipated into the rough surface in Fig. 2 can be obtained by evaluating the following integral:

$$P = -\frac{1}{2}\mathrm{Re}\left[\int (\mathbf{E} \times \mathbf{H}^*) \cdot \mathbf{a}_n \, dS\right] = -\frac{1}{2}\mathrm{Re}\left[\int \mathbf{H}^* \cdot (\mathbf{a}_y \times \mathbf{E}_n) \, dS\right]. \quad (2)$$

The integration in (2) could be carried out along the actual roughness profile, but since the dielectric region is lossless, could equally well be done over a plane surface located high enough above the rough surface that only the effective field [i.e., the field which enters into (1)] is required, rather than the total field, which also includes fine variations near the surface. If this is done, the integral using only effective fields can then be relocated to the effective smooth surface (i.e., the $y = 0$ plane) where the GIBC in (1) is enforced. By substituting the GIBC into (2), the following is obtained:

$$P = \frac{1}{2}\mu_d \omega p \left(\mathrm{Im}[\alpha_{mx}] \int |H_x|^2 \, dS + \mathrm{Im}[\alpha_{mz}] \int |H_z|^2 \, dS\right) + \frac{1}{2} p \alpha_{ey} \mathrm{Re}\left[\int \mathbf{H}^* \cdot (\mathbf{a}_y \times \nabla E_y) \, dS\right] \quad (3)$$

where μ_d ($= \mu_0 \mu_{rd}$) denotes the permeability of the dielectric region above the conductor. Following a similar procedure to

that used in [17], it can be shown that the last term in this expression is zero. Thus, the power dissipated into the rough interface is given by

$$P = \frac{1}{2}\mu_d \omega p \left(\mathrm{Im}[\alpha_{mx}] \int |H_x|^2 \, dS + \mathrm{Im}[\alpha_{mz}] \int |H_z|^2 \, dS \right). \quad (4)$$

For a smooth interface, the GIBC given in (1) can be shown [12] to reduce to the standard Leontovich condition (indeed, we think it rather remarkable that the Leontovich condition can be viewed in terms of complex magnetic polarizability densities). For a smooth interface, the magnetic polarizability densities are [12]

$$\alpha_{mz} = \alpha_{mx} = \frac{(j-1)}{2} \frac{\delta}{p} \frac{\mu_{rc}}{\mu_{rd}} \quad (5)$$

where μ_c $(= \mu_0 \mu_{rc})$ denotes the permeability of the conductor and $\delta = \sqrt{2/\omega \mu_c \sigma_c}$ is the skin depth. By substituting this into (4), the power dissipated into a smooth interface is given by the following:

$$P_o = \frac{1}{2}\mu_d \omega p \frac{\delta}{2p} \frac{\mu_{rc}}{\mu_{rd}} \left(\int |H_x|^2 \, dS + \int |H_z|^2 \, dS \right). \quad (6)$$

Thus, the ratio of the power loss of a rough conductor to that of the same conductor with a smooth surface is given by

$$\frac{P}{P_o} \sim 2\frac{p}{\delta} \frac{\mu_{rc}}{\mu_{rd}} \frac{\mathrm{Im}[\alpha_{mx}] \int |H_x|^2 \, dS + \mathrm{Im}[\alpha_{mz}] \int |H_z|^2 \, dS}{\int |H_x|^2 \, dS + \int |H_z|^2 \, dS}. \quad (7)$$

We will now separately consider the two possible polarizations of the current flow.

A. Power Loss Calculation for the Current Flowing Transverse to the Roughness Profile

The polarization corresponding to current flow transverse to the roughness profile has only a z-component of the H-field (we call this case an H-polarized wave) in (7). This leads to the following for the power loss ratio:

$$\frac{P}{P_o} \sim 2\frac{p}{\delta} \mathrm{Im}[\alpha_{mz}]. \quad (8)$$

In this analysis, it is assumed that $\mu_{rc} = \mu_{rd}$. In [12], it is shown that α_{mz} is expressed in terms of dimensionless parameters by the following:

$$\alpha_{mz} = -\left[S_o + \frac{1}{\mu_{rd}} \int_{B_c} \mathcal{B}_z \, dS_\xi \right]. \quad (9)$$

The parameter S_o is the area under the period cell (i.e., the shaded area between the conductor surface and $y = 0$ reference plane, as shown in Fig. 2), the integration is over the portion B_c of a period cell shown in Fig. 3, and $\mathcal{B}_z$ is a normalized periodic magnetic field in the conductor, which is governed by the following eddy current problem:

$$(\nabla_\xi^2 + G)\mathcal{H}_z = 0 \text{ in the conductor}$$

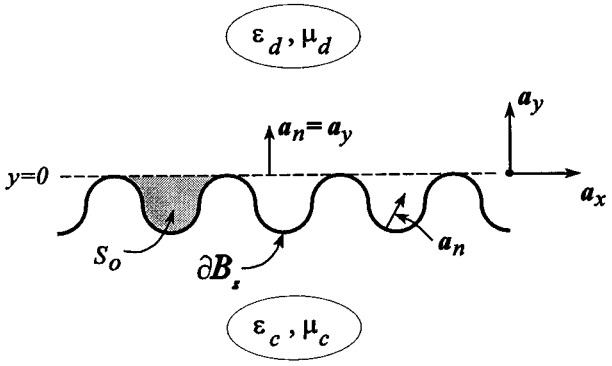

Fig. 2. Fictitious $y = 0$ plane along the top of the roughness profiles.

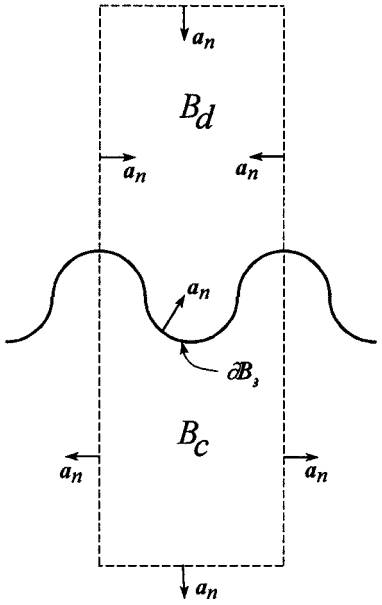

Fig. 3. Periodic cell.

$$\mathcal{H}_z = \frac{1}{\mu_{rc}} \mathcal{B}_z$$
$$\mathcal{H}_z|_{\partial B_s} = 1 \quad (10)$$

where ∂B_s is the roughness profile boundary (see Fig. 1). Here, $\boldsymbol{\xi}$ is a scaled dimensionless space variable defined by $\boldsymbol{\xi} = \mathbf{r}/p$ (see [12] and [16] for details) and G is the scaled wavenumber in the conducting region, which is expressed in terms of p/δ (see [12] for details) as

$$G = -j2\left(\frac{p}{\delta}\right)^2. \quad (11)$$

This is a straightforward boundary problem to solve numerically. In [18] and [19], a variational expression for $\int_{B_c} \mathcal{B}_z \, dS_\xi$ is given by

$$\frac{1}{\mu_{rd}} \int_{B_c} \mathcal{B}_z \, dS_\xi = \mathbf{a}_z \frac{W}{G}$$

where

$$W = \int (\nabla_\xi \mathcal{H}_z^{\mathrm{tr}})^2 \, dS_\xi - G \int (\mathcal{H}_z^{\mathrm{tr}})^2 \, dS_\xi \quad (12)$$

and $\mathcal{H}_z^{\mathrm{tr}}$ is a "trial" function.

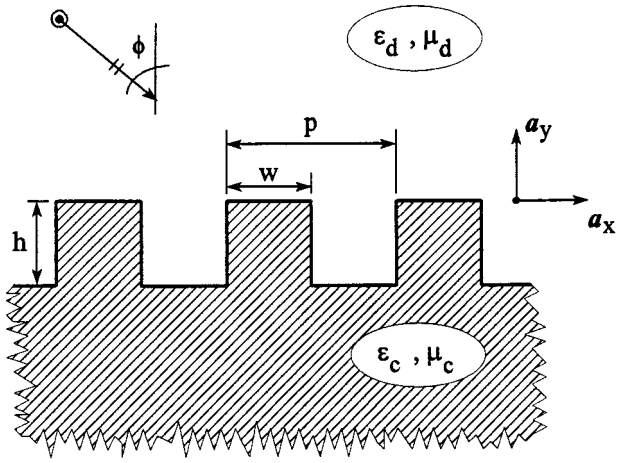

Fig. 4. Two-dimensional rectangular profile.

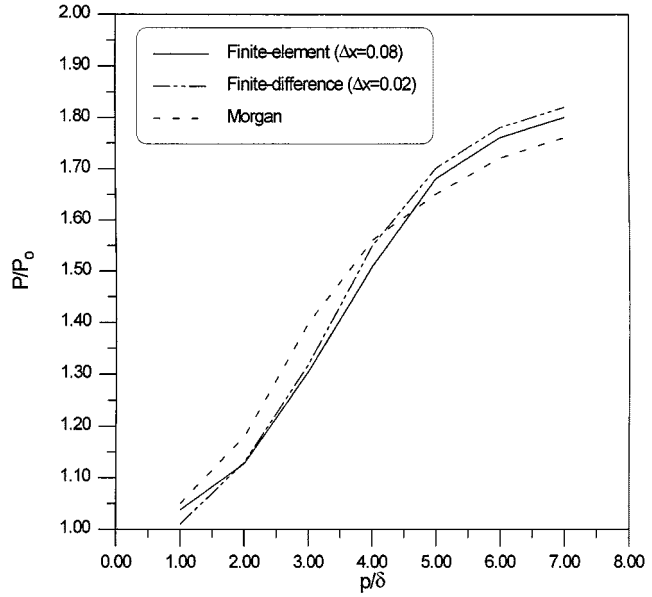

Fig. 5. Grooves transverse to current flow for $h/p = 0.5$ and $w/p = 0.5$.

In [18] and [19], the implementation of the finite-element method to determine the value of W for arbitrarily shaped roughness profiles is described. We have used this finite-element code to analyze a rectangular roughness profile for various h/p and w/p ratios (see Fig. 4). Fig. 5 shows the results for $h/p = 0.5$ and $w/p = 0.5$. Morgan, in his classic paper [20], analyzed this same polarization and geometry by the finite-difference method and the results are also shown in Fig. 5. The two sets of results are seen to be in fair agreement. A simpler alternative to the variational formulation for $\int_{B_c} \mathcal{B}_z \, dS_\xi$ is to solve for the fields with a finite-difference scheme. This is expected to be less accurate since it is not based on a variational formulation, but it is easier to implement. Results based on a finite-difference code are also shown in Fig. 5. It is seen that these results are comparable to the finite-element results, but required a grid size four times as small.

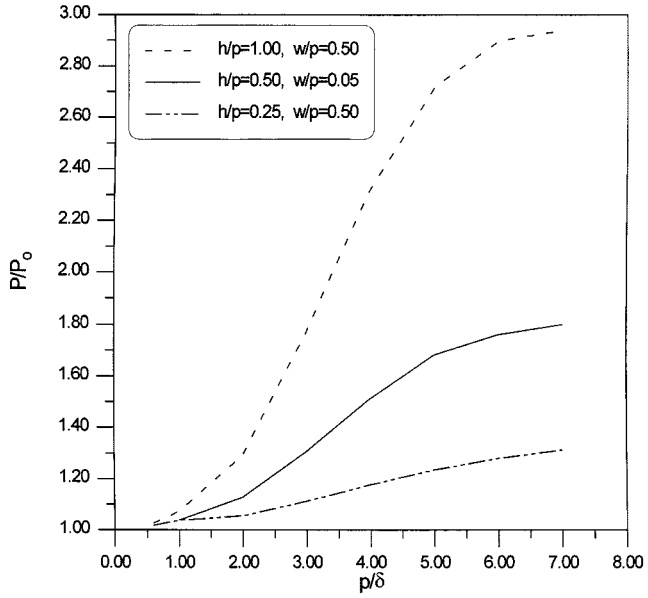

Fig. 6. Grooves transverse to current flow with $w/p = 0.5$ and h/p equal to 0.25, 0.5, and 1.0.

Fig. 5 shows that as $p/\delta \Rightarrow 0$ (the skin depth is large compared to the roughness dimensions), the ratio $P/P_o \Rightarrow 1$. This is expected based on our above discussion. On the other hand, as p/δ gets large, the currents are forced to follow the top of the roughness profile. The power loss ratio appears in all methods to approach an asymptotic value in this small skin depth limit. For this polarization, the asymptote is simply the relative increase in path length that the current must follow due to the roughness profile. For a rectangular profile with $h/p = 0.5$, the asymptote is two.

One important aspect of this paper is to determine which of the roughness characteristics contributes most to the power loss: the height, the width, or a combination of both. Fig. 6 shows results for $w/p = 0.5$ and three different values of h/p: 0.25, 0.5, and 1.0, respectively. Each of these curves approaches a different asymptote for the small skin depth limit. For h/p equal to 0.25, 0.5, and 1.0, the asymptotes appear to be 1.5, 2.0, and 3.0, respectively, as expected from the ratios of the path lengths on the rough surface to that of the smooth surface. Fig. 7 shows results for $h/p = 0.5$ and w/p equal to 0.25, 0.5, and 0.75. Again, as expected, all three curves approach the asymptote expected from the added path length in the small skin depth limit. Even though these three curves all approach the same asymptote, at any given p/δ, a profile with a larger top section has a larger loss. This seems to suggest that a major factor in determining power loss is the shape of the uppermost part of the roughness.

B. Power Loss Calculation for the Current Flowing Parallel to the Roughness Profile

An E-polarized wave (with the H-field polarized in the x-direction) has a power loss ratio of

$$\frac{P}{P_o} \sim 2\frac{p}{\delta}\mathrm{Im}[\alpha_{mx}] \tag{13}$$

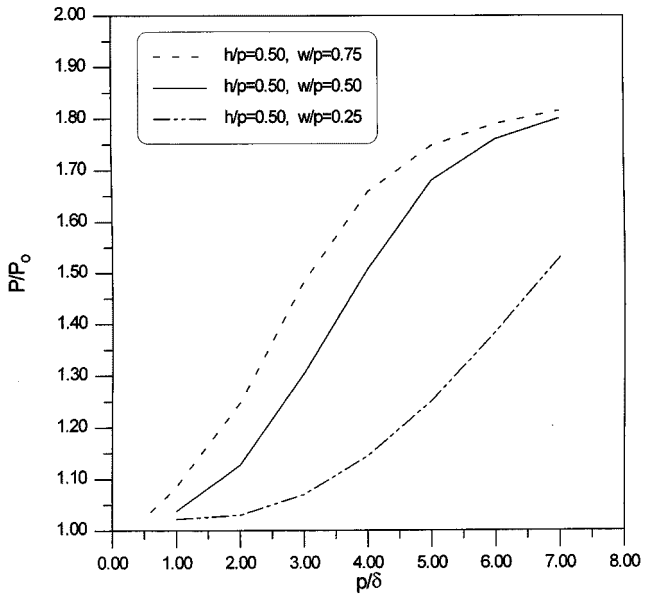

Fig. 7. Grooves transverse to current flow with $h/p = 0.5$ and w/p equal to 0.25, 0.5, and 0.75.

where again it is assumed that $\mu_{rc} = \mu_{rd}$. In [12], it is shown that α_{mx} is defined in terms of dimensionless parameters by the following:

$$\alpha_{mx} = -[S_o + \mathcal{I}] \tag{14}$$

where

$$\mathcal{I} = \frac{1}{\mu_{rd}} \left(\int_{B_d} \mathcal{B}_x \, dS_\xi + \int_{B_c} \mathcal{B}_x \, dS_\xi \right). \tag{15}$$

The parameter S_o is as before, and the integration is over the period cell in both the conductor and dielectric (shown in Fig. 3). $\mathcal{B}_x$ is a normalized periodic magnetic field, and for this polarization is the x-component of the field governed by the following eddy current problem:

$$\begin{aligned} \nabla_\xi \cdot \boldsymbol{\mathcal{B}}_d = 0 &\Rightarrow \xi \in B_d \\ \nabla_\xi \times \boldsymbol{\mathcal{H}}_d = 0 &\Rightarrow \xi \in B_d \\ (\nabla_\xi^2 + G)\boldsymbol{\mathcal{H}}_c = 0 &\Rightarrow \xi \in B_c \end{aligned} \tag{16}$$

with constitutive equations

$$\begin{aligned} \boldsymbol{\mathcal{B}}_d = \mu_{rd}\boldsymbol{\mathcal{H}}_d &\Rightarrow \xi \in B_d \\ \boldsymbol{\mathcal{B}}_c = \mu_{rc}\boldsymbol{\mathcal{H}}_d &\Rightarrow \xi \in B_c \end{aligned} \tag{17}$$

and boundary conditions

$$\begin{aligned} \mathbf{a}_n \times (\boldsymbol{\mathcal{H}}_d|_{\xi\in\partial B_s} - \boldsymbol{\mathcal{H}}_c|_{\xi\in\partial B_s}) &= -\mathbf{a}_n \times \mathbf{a}_x \\ \mathbf{a}_n \cdot (\boldsymbol{\mathcal{B}}_d|_{\xi\in\partial B_s} - \boldsymbol{\mathcal{B}}_c|_{\xi\in\partial B_s}) &= -\mu_{rd}\mathbf{a}_n \cdot \mathbf{a}_x \end{aligned} \tag{18}$$

where the subscripts d and c indicate the dielectric and conductor regions, respectively.

In this polarization, the fields in both the dielectric and conductor are needed to determine α_{mx} and, as a result, this is a more complicated boundary problem to solve than in the other polarization. Especially for numerical purposes, it is more convenient to solve for the potential A_c and A_d. It can be shown ([18] and [19]) that the these vector potentials are governed by the following equations:

$$\begin{aligned} \nabla_\xi^2 A_d = 0 &\Rightarrow \text{defined in the dielectric} \\ (\nabla_\xi^2 + G)A_c = 0 &\Rightarrow \text{defined in the conductor} \end{aligned} \tag{19}$$

where G is defined in (11). The boundary conditions for these potentials are

$$\begin{aligned} A_c - A_d = \mathcal{V} &\equiv \xi_y|_{\partial B_s} \\ \mathbf{a}_n \cdot \nabla_\xi A_c - \mathbf{a}_n \cdot \nabla_\xi A_d = \mathcal{D} &\equiv \mathbf{a}_n \cdot \mathbf{a}_y|_{\partial B_s}. \end{aligned} \tag{20}$$

A variational expression for $\mathcal{I}$ is given by [18], [19]

$$\mathcal{I} = W \tag{21}$$

where

$$\begin{aligned} W = &\int (\nabla_\xi A^{\mathrm{tr}})^2 \, dS_\xi - k^2 G \int (A_c^{\mathrm{tr}})^2 \, dS_\xi \\ &- \int (A_c^{\mathrm{tr}} + A_d^{\mathrm{tr}})\mathcal{D} \, dl_\xi \\ &- \int (\mathbf{a}_n \cdot \nabla_\xi A_c^{\mathrm{tr}} + \mathbf{a}_n \cdot \nabla_\xi A_d^{\mathrm{tr}})\mathcal{V} \, dl_\xi \\ &- \int (A_c^{\mathrm{tr}} - A_d^{\mathrm{tr}})\mathbf{a}_n \cdot \nabla_\xi A_c^{\mathrm{tr}} \, dl_\xi \\ &- \int (A_c^{\mathrm{tr}} - A_d^{\mathrm{tr}})\mathbf{a}_n \cdot \nabla_\xi A_d^{\mathrm{tr}} \, dl_\xi, \end{aligned} \tag{22}$$

where $\mathcal{D}$ and $\mathcal{V}$ are defined in (20).

References [18] and [19] also describe the use of finite elements to numerically determine the value of W for an arbitrarily shaped roughness profile. The resulting code was used to analyze a rectangular profile for different h/p and w/p ratios. Fig. 8 shows results for $h/p = 0.5$ and $w/p = 0.5$. As p/δ approaches zero, the power loss ratio approaches one, as expected. The ratio exhibits a sort of resonance behavior with a peak at $p/\delta = 4$ and a broad valley at $p/\delta = 8$. From this minimum out to the very small skin depth limit, the loss appears to approach some asymptotic limit. Unlike for the other polarization, Morgan did not present numerical results for this case, but by using a standard wall loss perturbation procedure, he was able to determine a high-frequency asymptote. For this geometry Morgan's calculated asymptote is 1.36. The numerical results presented here appear to approach that value.

As with the other polarization, it is important to determine which of the roughness characteristics contributes most to the power loss. Fig. 9 shows results for $w/p = 0.5$ and h/p equal to 0.25, 0.5, and 1.0. Even for $p/\delta = 16$, it is not yet clear what the asymptotic values of the power ratio will be, but they will clearly not differ greatly from each other in the three cases examined here. Fig. 10 shows results for $h/p = 0.5$ and w/p equal to 0.25, 0.5, and 0.75. Each curve now appears to be approaching a different asymptote in the small skin depth limit: for $w/p = 0.75$, this asymptote is less than 1.2, while for $w/p = 0.5$ and 0.25, its value is significantly larger. When w/p is large, the fields do not penetrate very deeply into the trough because they must do so essentially as TM modes of the parallel-plate waveguide formed by the vertical walls, and these modes are cutoff. As w/p gets smaller, the fields penetrate more deeply into the trough, "seeing" more lossy wall surface and,

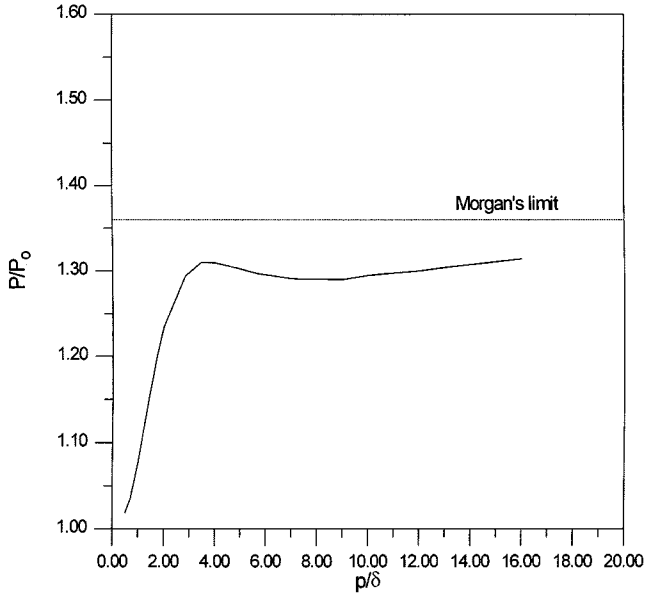

Fig. 8. Grooves parallel to current flow for $h/p = 0.5$ and $w/p = 0.5$.

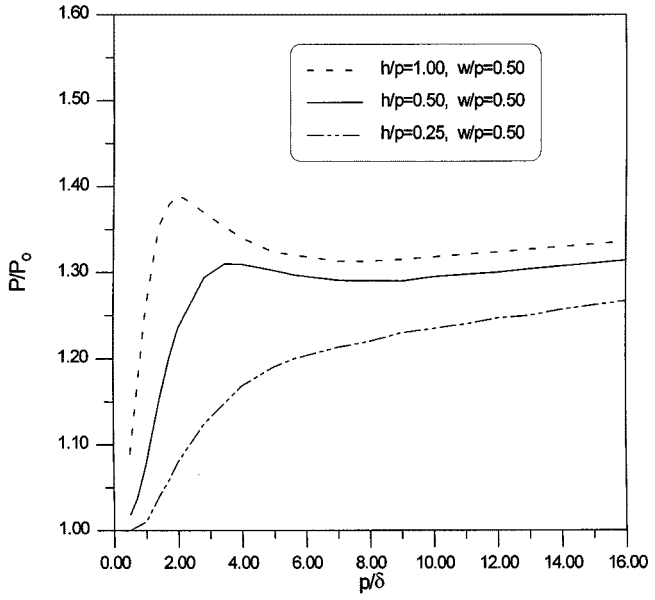

Fig. 9. Grooves parallel to current flow with $w/p = 0.5$ and h/p equal to 0.25, 0.5, and 1.0.

thus, resulting in greater loss. In addition, the smaller w/p becomes, the more pronounced the resonance behavior becomes. This may be due to the partial reflection of a TM waveguide mode from the bottom wall of the trough region. In any case, it appears that, for this polarization, the width of the roughness has a greater effect on the power loss than does the height.

III. Power Loss Calculations for a Two-Dimensional Rough Superconductor

In this section, the additional power loss at a rough superconductor for the currents flowing parallel to the roughness is presented. There has been some work in the past on the subject of roughness effects in superconducting materials [21]–[24]. The theory presented in this paper is general enough to handle both standard conductors as well as superconductors, thus, a comparison will be made to the results in the literature for superconducting materials. Only the case when the roughness troughs are parallel to the current flow will be considered in detail here.

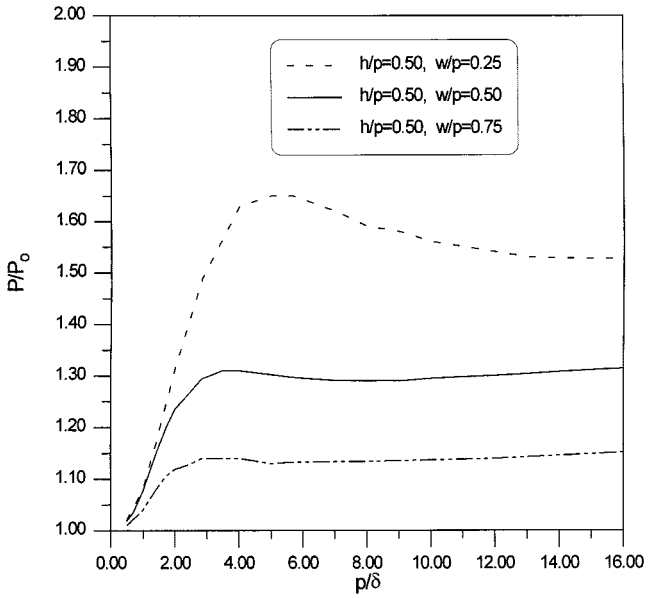

Fig. 10. Grooves parallel to current flow with $h/p = 0.5$ and w/p equal to 0.25, 0.5, and 0.75.

A superconductor can be characterized similarly to a standard conductor by replacing the original conductivity σ by a complex conductivity, which results in a complex skin depth [25]–[27] given by

$$\delta_{sc} = \frac{\delta}{\sqrt{1 + \dfrac{\delta^2}{2j\lambda^2}}} \tag{23}$$

where δ is the skin depth for a standard conductor and λ is the London superconductor penetration depth. δ_{sc} is dominated by the smaller of the two quantities δ and λ. For the standard conductor, $\lambda \to \infty$ and $\delta_{sc} = \delta$.

To solve for α_{mx} for a rough superconducting surface, the fields in the superconductor must be found, which requires the scaled wavenumber for a superconductor. This quantity is obtained by replacing the standard conductor skin depth in (11) by the superconductor skin depth given in (23), which gives

$$G = -j2\left(\frac{p}{\delta_{sc}}\right)^2 = -j2\left(\frac{p}{\delta}\right)^2\left[1 + \frac{\delta^2}{2j\lambda^2}\right]. \tag{24}$$

The magnetic polarizability density for a smooth superconductor is found either by obtaining the H-field in a smooth superconductor (see [25]–[27] for details) and then evaluating the integral in (15) or by simply replacing the standard conductor skin depth in (5) by the superconductor skin depth given in (23).

Either approach gives the following for the magnetic polarizability densities for a smooth superconductor:

$$\alpha_{mz} = \alpha_{mx} = \frac{(j-1)}{2}\,\frac{\delta}{p}\,\frac{1}{\sqrt{1+\dfrac{\delta^2}{2j\lambda^2}}}. \tag{25}$$

In the limit of a standard conductor ($\lambda \to \infty$), this expression reduces to (5). The power loss ratio for E-polarized fields is then

$$\frac{P}{P_o} \sim 2\frac{p}{\delta}\,\frac{\mathrm{Im}[\alpha_{mx}]}{\mathrm{Im}\left[\dfrac{j-1}{\sqrt{1+\dfrac{\delta^2}{2j\lambda^2}}}\right]}. \tag{26}$$

In the limit of a standard conductor ($\lambda \to \infty$), this expression reduces to (13).

For good superconductors, $\delta \gg \lambda$ and the power loss ratio becomes

$$\frac{P}{P_o} \sim \frac{p}{\lambda}\left(\frac{\delta^2}{\lambda^2}\right)\mathrm{Im}[\alpha_{mx}]. \tag{27}$$

Results for a rectangular superconducting surface with $h/p = 0.5$ and $w/p = 0.5$ with $\delta = 10\lambda$ are shown in Fig. 11. This case was treated by Mende and Spitsyn [24], and these results are also shown in Fig. 11. As seen by the curves, the two results agree well with one another.

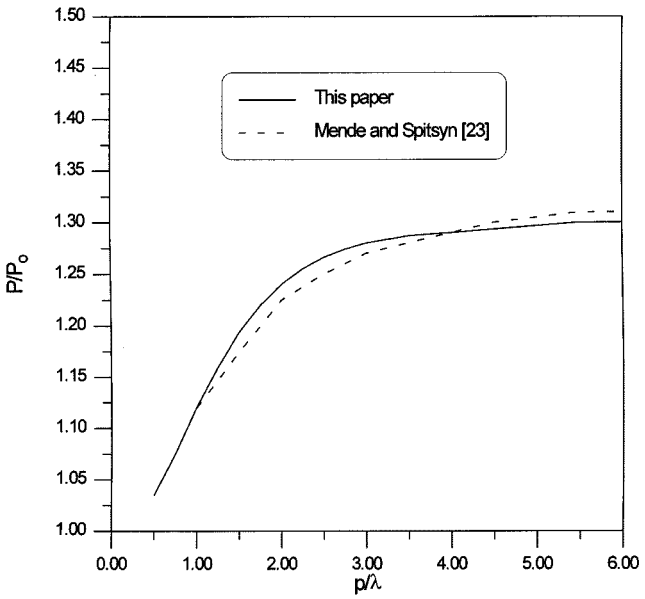

Fig. 11. Loss calculation for a superconducting interface for $w/p = 0.5$ and $h/p = 0.5$.

IV. Approximations of the Power Loss

In the previous three sections, we showed that numerical results based on a variational formulation used in this paper agree well with other published data. We will next attempt to obtain simple analytical expressions for the power loss by making relatively crude approximations for the fields in the variational expressions for W. This approach would eliminate the need for determining W numerically. In this section, two different approximations to the fields are used to determine if this is indeed possible.

In this section, we consider only the polarization for which the grooves are parallel to the current flow. In this case, it is more convenient to work with the potentials A_c and A_d. The first approximation assumes that the potentials in the dielectric and conductor region are nearly those for the case of a planar interface. These are constant in the dielectric region, and exhibit the following exponential decay in the conductor:

$$\begin{aligned} A_d^{\mathrm{tr}} &= C_1 \\ A_c^{\mathrm{tr}} &= C_2 e^{-\Gamma_o y} \end{aligned} \tag{28}$$

where

$$\Gamma_o = j\sqrt{G}.$$

These expressions for the potentials can be substituted into (22), and the resulting integrals evaluated over the actual roughness profile. Once this is done, an expression for W in terms of the two unknown constants can be obtained. By applying the standard Rayleigh–Ritz procedure, the unknown constants C_1 and C_2 can then be determined from

$$\begin{aligned} \frac{\partial W}{\partial C_1} &= 0 \\ \frac{\partial W}{\partial C_2} &= 0. \end{aligned}$$

This results in the following expression for W for a rectangular profile with $w/p = 0.5$ and $h/p = 0.25$:

$$W = -\left[\frac{1}{\Gamma_o} + h\frac{e^{-\Gamma_o h}}{(1+e^{-\Gamma_o h})}\right]. \tag{29}$$

The first term is the flat surface value of W (what W would be for a smooth interface), and the second term is a correction. Fig. 12 shows the results using (29) to determine the power loss ratio. Also plotted in this figure are numerical results. For $p/\delta < 2$, this approximation shows fairly good agreement. However, for larger values of p/δ, the approximation significantly overshoots the numerical results.

The second approximation (which we will refer to as RR) is based on the Rayleigh–Rice perturbation procedure [28], [29]. The basic idea is to assume that the slope, or the height h, of the roughness is small, such that the potentials in both regions can be expanded in a series in increasing powers of h as

$$\begin{aligned} A_c &\sim A_c^o + hA_c^1 + O(h^2) \\ A_d &\sim A_d^o + hA_d^1 + O(h^2). \end{aligned}$$

Substituting these into (19) and (20), and grouping like powers of h, we obtain

$$A_d^{\mathrm{tr}} = C_1\left[\frac{1}{\Gamma_o} - h\Gamma_o\sum_{n=1}^{\infty}\frac{e^{-\alpha_n y}}{\alpha_n+\Gamma_n} \cdot\left\{f_{cn}\cos(\alpha_n x) + f_{sn}\sin(\alpha_n x)\right\}\right] \tag{30}$$

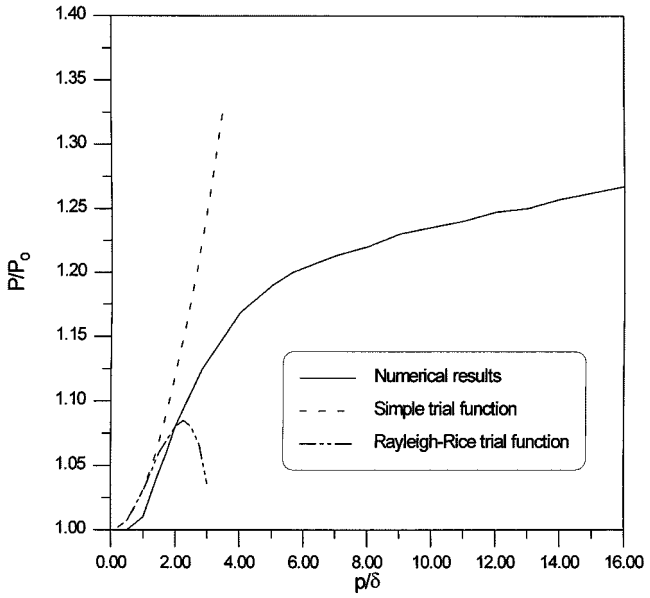

Fig. 12. Approximation for the power loss for a rectangular profile for $w/p = 0.5$ and $h/p = 0.25$.

and

$$A_c^{\text{tr}} = C_2 \left[\frac{e^{-\Gamma_o y}}{\Gamma_o} - h\Gamma_o \sum_{n=1}^{\infty} \frac{e^{-\Gamma_n y}}{\alpha_n + \Gamma_n} \cdot \left\{ f_{cn} \cos(\alpha_n x) + f_{sn} \sin(\alpha_n x) \right\} \right] \quad (31)$$

where

$$\alpha_n = 2\pi n \quad \Gamma_n = \sqrt{\alpha_n^2 + \Gamma_o^2}.$$

The expressions for A_c and A_d given in (30) and (31) are now used as trial functions in the expression for W given in (22). The unknown constants C_1 and C_2 are again determined by the Rayleigh–Ritz procedure. We wish to emphasize that our "RR" method is *not* the same as the classic Rayleigh–Rice technique, but merely uses the fields of the latter as trial fields in a variational expression.

The resulting value for W in the RR method is rather involved and is not given here. However, results for $w/p = 0.5$ and $h/p = 0.25$ are shown in Fig. 12. When $p/\delta < 1.5$, our two approximations are essentially the same. For larger values of p/δ, the RR approximation tries to correct for the overshoot seen in the flat surface approximation. However, the RR procedure eventually overcorrects and produces values much less than the numerical results.

For $p/\delta < 2$, both of these approaches give good results, but for $p/\delta > 2.5$, even the RR procedure fails. The problem with the RR approximation is that the slope is not small for a rectangular profile; rather, the slope is, in places, infinite. A better trial field would be needed to achieve more accurate results. For profiles that are not so steep (say, sawtoothed or sinusoidal) the RR approximation may indeed be a viable alternative, and this will be the topic of future research.

V. Discussion and Conclusion

In this paper, we use a previously derived impedance-type boundary condition to analyze the effects of surface roughness on the power loss in MIMICs. We have shown that the results in this paper correlate very well with other published results.

The purpose of this paper was to determine whether surface roughness will significantly affect the power loss associated with planar circuits. We have shown that, as the roughness dimensions get large compared to the skin depth, there are indeed noticeable roughness effects. Thus, the practical question to ask is: What are typical values for p/δ associated with MIMICs? Most MIMICs are currently fabricated on GaAs; in Section I, we showed that common roughness dimensions on quality materials are on the order of 100 Å. With present technology, one cannot expect MIMIC circuits to operate at frequencies much higher than a few hundred gigahertz, say, $f_{\max} = 200$ GHz. Therefore, one should expect the ratio $(p/\delta)_{\max}$ to be on the order of 0.05. In the analysis of the two-dimensional periodic roughness, we showed that, for p/δ in this range, negligible additional power loss results.

Typical surface roughness cannot in reality be represented accurately by two-dimensional periodic profiles, but are instead more likely to have three-dimensional random profiles. For the very small p/δ ratio, which is usually seen on GaAs substrates, there is no physical reason to expect that the more general random profiles will exhibit drastically different P/P_o behavior from that of the two-dimensional periodic surfaces. As a result, we conclude that for MIMICs fabricated on most commercial available GaAs substrates, surface roughness effects are negligible and, for the most part, can be ignored.

Although the above roughness dimensions for GaAs are the general rule, exceptions do exist. Mickelson [32] has shown that on some very thin commercially available GaAs wafers, the roughness parameter p/δ can be on the order of 1–6, and he has observed loss increases in this material compared to other GaAs wafers. It is believed that these large roughness dimensions were the result of the polishing process for certain less expensive GaAs wafers.

The situation is quite different if circuits are fabricated on PTFE and Al_2O_3. For these kinds of substrates and the metallization procedures used with them, roughness dimensions are expected to be on the order of 1 μm. At typical microwave and millimeter-wave frequencies, this corresponds to a p/δ value ranging from 1 to 6. From our analysis of two-dimensional roughness, we see that under such conditions, the additional power loss resulting from a rough interface can be significant.

At these relatively large values of p/δ, the additional power loss associated with a randomly rough surface is also expected to be significant. However, quantitative predictions of this loss cannot be made from our analysis of the two-dimensional profiles. The random profiles will have different contributions from the different possible polarizations of the incident fields. Therefore, for planar circuits fabricated on PTFE and Al_2O_3, future work is needed to handle these more realistic random surfaces.

Random roughness profiles can be analyzed in different ways. The first is based on the periodic analysis performed in [12].

Even though the true surface is randomly rough, there will be no major variation of the roughness along the surface. That is to say, for most processes, the roughness will have an rms height, and the peaks and valleys of the roughness will be on the same order along the whole surface and will be local to the rms height. Therefore, for a random surface, one could choose a small portion of the surface that is typical of the total surface profile and then assume that the surface is periodic with the profiles of one period being that of the small portion chosen. With this quasi-periodic surface, the procedure shown in [12] can be used. The width of this quasi-periodic surface needs to be small compared to a wavelength and other circuit dimensions, as discussed in [16].

Another approach involves analyzing the random roughness directly. The first approach is based on the Rayleigh–Rice technique. Research by Sanderson [28] shows that the Rayleigh–Rice perturbation technique gives good results for periodic surface roughness whose slopes are small to moderate. Sanderson [28] and Rytov *et al*. [33] speculate that this may also be true for random or nonperiodic roughness. It is believed then, that the Rayleigh–Rice theory could be used to obtain an impedance boundary condition for such random roughness profiles.

A third approach would be based on the work by Biot [30], [31], Twersky [34], and Wait [35]. This technique involves replacing a typical roughness "bump" (or boss) by the induced dipole electric moment caused by an incident field onto the boss. By summing over all the induced dipoles caused by randomly shaped bosses at random intervals, it may be possible to determine an effective impedance boundary condition for the randomly rough profile.

However, no matter what technique is used to treat the case of random roughness, we must first extend the solution to handle the three-dimensional problem. Most importantly, a general three-dimensional periodic eddy current solver must be developed before we can hope to tackle random roughness profiles.

The results in this paper were obtained using a previously derived impedance boundary condition [12]. This boundary condition is such that it can be implemented into numerical codes to analyze roughness effects. A similar surface impedance obtained for edge shape effects has been implemented in a moment-method code [6]. In closing, the research presented here is general enough to allow the analysis of conductors with multiple-metallization layers (commonly found in MIMIC circuits). This will be the topic of a future paper.

REFERENCES

[1] R. K. Hoffmann, *Handbook of Microwave Integrated Circuits*. Norwood, MA: Artech House, 1987.

[2] K. C. Gupta, R. Garg, and I. J. Bahl, *Microstrip Lines and Slotlines*. Norwood, MA: Artech House, 1979.

[3] J. R. Brews, "Transmission line models for lossy waveguide interconnections in VLSI," *IEEE Trans. Electron Devices*, vol. ED-33, pp. 1356–1365, Sept. 1986.

[4] T. C. Edwards, *Foundations for Microstrip Circuit Design*. New York: Wiley, 1981.

[5] M. A. Leontovich, "Approximate boundary conditions for electromagnetic fields at the surface of a highly conducting body" (in Russian), in *Issledovaniya po Rasprostraneniyu Radiovoln*. Moscow, Russia: Nauka, 1948, pt. 2, pp. 5–12.

[6] ——, *Izbrannye Trudy: Teoreticheskaya Fizika*, M. A. Leontovich, Ed. Moscow, Russia: Nauka, 1985, pp. 351–355.

[7] C. L. Holloway and E. F. Kuester, "Edge shape effects and quasiclosed form expressions for the conductor loss of microstrip lines," *Radio Sci.*, vol. 29, pp. 539–559, 1994.

[8] ——, "A quasi-closed form expression for the conductor loss of CPW lines, with an investigation of edge shape effects," *IEEE Trans. Microwave Theory Tech.*, vol. 43, pp. 2695–2701, Dec. 1995.

[9] *Design Guide for PTFE-Based Circuit Boards*: Soladyne Div., Rogers, 1991.

[10] *Metallization Bulletin*: Trans-Tech Inc., Alpha, 1991.

[11] *Trans-Strates Microwave Substrates*: Trans-Tech Inc., Alpha, 1990.

[12] C. L. Holloway and E. F. Kuester, "Impedance-type boundary conditions for a periodic interface between a dielectric and highly conducting medium," *IEEE Trans. Antennas Propagat.*, vol. 48, Oct. 2000, to be published.

[13] R. Garcia-Molina, A. A. Maradudin, and T. A. Leskova, "The impedance boundary condition for a curved surface," *Phys. Reps.*, vol. 194, pp. 351–359, 1990.

[14] A. A. Maradudin, "The impedance boundary condition for a one-dimensional, curved, metal surface," *Opt. Commun.*, vol. 103, pp. 227–234, 1993.

[15] ——, "The impedance boundary condition at a two-dimensional rough metal surface," *Opt. Commun.*, vol. 116, pp. 452–467, 1995.

[16] C. L. Holloway and E. F. Kuester, "Equivalent boundary conditions for a perfectly conducting periodic surface with a cover layer," *Radio Sci.*, vol. 35, no. 3, pp. 661–681, 2000.

[17] T. B. A. Senior and J. L. Volakis, *Approximate Boundary Conditions in Electromagnetics*. London, U.K.: IEE Press, 1995, ch. 5, pp. 180–182.

[18] C. L. Holloway and E. F. Kuester, "A variational formulation for a general class of eddy current problem", to be published.

[19] C. L. Holloway, "Edge and surface shape effects on conductor loss asso ciated with planar circuits," Electromag. Lab., Dept. Elect. Comput. Eng., Univ. Colorado, Boulder, CO, MIMICAD Tech Rep., 1992.

[20] S. P. Morgan, "Effect of surface roughness on eddy current losses at microwave frequencies," *J. Appl. Phys.*, vol. 20, pp. 352–362, 1949.

[21] F. F. Mende, A. I. Spitsyn, and V. N. Podlesnyi, "Effect of roughness on surface impedance and effective penetration depth in superconductors," *Sov. Phys.—Tech. Phys.*, vol. 26, no. 12, pp. 1512–1515, 1982.

[22] F. F. Mende, A. I. Spitsyn, N. A. Kochkonyan, and A. V. Skugarevski, "Surface impedance of real superconducting surfaces," *Cryogen.*, pp. 10–12, Jan. 1985.

[23] Z. Wu and L. E. Davis, "Surface roughness effect on surface impedance of superconductors," *J. Appl. Phys.*, vol. 76, pp. 3669–3672, 1994.

[24] F. F. Mende and A. I. Spitsyn, *Poverkhnostnyi Impedans Sverkhprovodnikov*. Kiev, Ukraine: Naukova Dumka, 1985, ch. 3.

[25] R. E. Matick, *Transmission Lines for Digital and Communication Networks*. New York: McGraw-Hill, 1969, ch. 6.

[26] L. D. Landau and E. M. Lifshitz, *Electrodynamics of Continuous Media*. New York: Pergamon, 1984.

[27] J. H. Hinken, *Superconductor Electronics*. Berlin, Germany: Springer-Verlag, 1989.

[28] A. E. Sanderson, "Effect of surface roughness on propagation of the TEM mode," in *Advances in Microwaves*, L. Young, Ed. New York: Academic, 1971, vol. 7, pp. 1–57.

[29] A. Ishimaru, *Electromagnetic Wave Propagation, Radiation and Scattering*. Englewood Cliffs, NJ: Prentice-Hall, 1991, ch. 7.

[30] M. A. Biot, "Some new aspects of the reflection of electromagnetic waves on a rough surface," *J. Appl. Phys.*, vol. 28, pp. 1455–1463, 1957.

[31] ——, "On the reflection of electromagnetic waves on a rough surface," *J. Appl. Phys.*, vol. 29, p. 998, 1958.

[32] A. R. Mickelson, private communication.

[33] S. M. Rytov, Y. A. Kravtsov, and V. I. Tatarskii, *Principles of Statistical Radiophysics 4: Wave Propagation Through Random Media*. Berlin, Germany: Springer-Verlag, 1989, ch. 5.

[34] V. Twersky, "On scattering and reflection of electromagnetic waves by rough surfaces," *IRE Trans. Antennas Propagat.*, vol. 5, pp. 81–90, Jan. 1957.

[35] J. R. Wait, "Guiding of electromagnetic waves by uniformly rough surfaces—Part I," *IRE Trans. Antennas Propagat.*, vol. 7, pp. S154–S162, Dec. 1959.

Christopher L. Holloway (S'86–M'92) was born in Chattanooga, TN, on March 26, 1962. He received the B.S. degree from the University of Tennessee at Chattanooga, in 1986, and the M.S. and Ph.D. degrees from the University of Colorado at Boulder, in 1988 and 1992, respectively, both in electrical engineering.

During 1992, he was a Research Scientist with Electro Magnetic Applications Inc., Lakewood, CO, where his responsibilities included theoretical analysis and finite-difference time-domain modeling of various electromagnetic problems. From the fall of 1992 to 1994, he was with the National Center for Atmospheric Research (NCAR), Boulder, CO, where his duties included wave-propagation modeling, signal-processing studies, and radar systems design. From 1994 to 2000, he was with the Institute for Telecommunication Sciences (ITS), U.S. Department of Commerce, Boulder, CO, where he was involved in wave-propagation studies. Since 2000, he has been with the National Institute of Standards and Technology (NIST), Boulder, CO, where he is involved with electromagnetic theory. He is also on the Graduate Faculty at the University of Colorado at Boulder. His research interests include electromagnetic-field theory, wave propagation, guided wave structures, remote sensing, numerical methods, and electromagnetic compatibility (EMC)/electromagnetic interference (EMI) issues.

Dr. Holloway is a member of the International Union of Radio Science (URSI) Commission A. He is an associate editor on propagation for the IEEE TRANSACTIONS ON ELECTROMAGNETIC COMPATIBILITY. He was the recipient of the 1999 Department of Commerce Silver Medal for his work in electromagnetic theory, and the 1998 Department of Commerce Bronze Medal for his work on printed circuit boards.

Edward F. Kuester (S'73–M-76–SM'95–F'98) was born in St. Louis, MO, on June 21, 1950. He received the B.S. degree from Michigan State University, East Lansing, in 1971, and the M.S. and Ph.D. degrees from the University of Colorado at Boulder, in 1974 and 1976, respectively, all in electrical engineering.

Since 1976, he has been a faculty member in the Department of Electrical and Computer Engineering, University of Colorado at Boulder, where he is currently a Professor. In 1979, he was a Summer Fellow at the Jet Propulsion Laboratory, California Institute of Technology, Pasadena. From 1981 to 1982, he was a Visiting Professor at the Technische Hogeschool, Delft, The Netherlands. During the 1992–1993 academic year, he was Professur Invité at the École Polytechnique Fédérale de Lausanne, Lausanne, Switzerland. His research interests include the electromagnetic theory of waveguiding and radiating structures at all frequencies, applied mathematics, and applied physics.

Prof. Kuester is a member of the International Union of Radio Science (URSI) Commission B and the Society for Industrial and Applied Mathematics (SIAM).